ARTICLES
https://doi.org/10.1038/s41561-019-0312-z
nature geoscience

Higher resilience to climatic disturbances in tropical vegetation exposed to more variable rainfall

Catrin Ciemer[1,2*], Niklas Boers[1,3], Marina Hirota[4,5], Jürgen Kurths[1,2,6], Finn Müller-Hansen[1,2], Rafael S. Oliveira[5] and Ricarda Winkelmann[1,7*]

With ongoing global warming, the amount and frequency of precipitation in the tropics is projected to change substantially. While it has been shown that tropical forests and savannahs are sustained within the same intermediate mean annual precipitation range, the mechanisms that lead to the resilience of these ecosystems are still not fully understood. In particular, the long-term impact of rainfall variability on resilience is as yet unclear. Here we present observational evidence that both tropical forest and savannah exposed to a higher rainfall variability—in particular on interannual scales—during their long-term past are overall more resilient against climatic disturbances. Based on precipitation and tree cover data in the Brazilian Amazon basin, we constructed potential landscapes that enable us to systematically measure the resilience of the different ecosystems. Additionally, we infer that shifts from forest to savannah due to decreasing precipitation in the future are more likely to occur in regions with a precursory lower rainfall variability. Long-term rainfall variability thus needs to be taken into account in resilience analyses and projections of vegetation response to climate change.

The Amazon rainforest has been projected to be at risk of large-scale dieback under future human influences and global climate change[1–3]. Even a partial forest dieback could cause a severe reduction in CO_2 uptake and hence a vast decline in global carbon storage[4,5]. This may, through a positive feedback loop, lead to a further acceleration of global warming[6]. The resilience[7–9] and the future development of the Amazon rainforest are therefore crucial to the discussion on climate mitigation and adaptation. Climate model projections suggest more prolonged droughts and thus an increase in water deficits in the Amazon basin in the future[10]. As the forest is highly dependent on water availability[11,12], prolonged droughts are likely to increase tree mortality and fire risk[13,14]. The projected changes in climate thus strongly favour transitions from forest to savannah ecosystems. In addition, tree cover has been reported to decrease with higher interannual rainfall variability in the wet tropics, whereas the opposite effect has been suggested for drier regions[15,16].

Here we analyse the effect of long-term rainfall variability on shaping the resilience of tropical forest and savannah to evaluate further how this effect may influence the response of the vegetation to future changes in the mean annual precipitation (MAP) predicted by the Intergovernmental Panel on Climate Change climate models[17]. For our analysis, we used high-resolution, satellite-derived continuous tree cover data (Moderate Resolution Imaging Spectroradiometer (MODIS) MOD44B[18] (Fig. 1a)) in combination with a station-based rainfall data set (Climate Research Unit (CRU)[19], see Methods and Supplementary Fig. 1). For a comparison with the satellite-derived TRMM 3B42 data set see Supplementary Fig. 2. As we evaluated natural ecosystems, it is essential to exclude areas that are already disturbed by human influences from the analyses. Therefore, we restricted our study area to tropical Brazil, for which highly accurate land use data are available (Fig. 1a).

Rainfall variability

Distinct vegetation states are dominant for particular MAP ranges. For precipitation levels above 2,100 mm yr^{-1}, the natural vegetation is almost exclusively lowland tropical forest, whereas savannah with sparse tree cover dominates regions with precipitation values below 1,300 mm yr^{-1}. For values in between these bounds (1,300 mm yr^{-1} < MAP < 2,100 mm yr^{-1}), both forest and savannah can be maintained (Supplementary Figs. 3 and 4). In this bistable precipitation range, shifts from the forest to the savannah state can be triggered by pulse-like disturbances, such as extreme droughts and fires, whereas a shift from the savannah to the forest state is rather smooth.

We aim to explore the overarching, long-term effect of rainfall variability on tropical vegetation stability. We determined distinct climatic regions for tropical Brazil, based on the seasonality and interannual variability of rainfall (see Fig. 3d,g and Supplementary Methods 1). Northwestern Brazil, which includes the remote part of the Amazon rainforest, shows a relatively low rainfall variability, whereas precipitation varies more strongly in eastern Brazil and close to Bolivia and Venezuela, both intra- and interannually (Fig. 1b). Generally, the ends of the spectrum, that is, very high and very low long-term rainfall variability, occur only in regions covered completely by either forest or savannah. As we wanted to study critical transition areas between the two vegetation states, we focused only on areas with intermediate long-term rainfall variability.

For these areas, bimodality in tree cover distributions hints at potential bistability[20] (Supplementary Fig. 3) using a space-for-time

[1]Potsdam Institute for Climate Impact Research, Potsdam, Germany. [2]Department of Physics, Humboldt University, Berlin, Germany. [3]Grantham Institute - Climate Change and the Environment, Imperial College London, London, UK. [4]Department of Physics, Federal University of Santa Catarina, Florianópolis, Brazil. [5]Institute of Biology, University of Campinas, Campinas, Brazil. [6]Saratov State University, Saratov, Russia. [7]Physics Institute, University of Potsdam, Potsdam, Germany. *e-mail: catrin.ciemer@pik-potsdam.de; ricarda.winkelmann@pik-potsdam.de

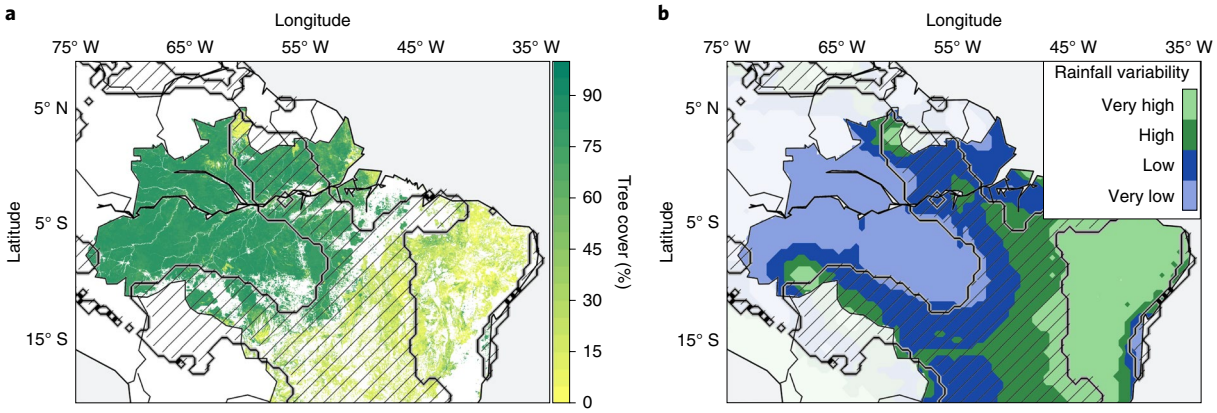

Fig. 1 | Bistable regions of rainforest and savannah. a, Spatial distribution of tree cover in the study area. Large coherent regions of high tree cover (around 75% tree cover) indicate the Amazon rainforest, whereas savannah is represented by low tree cover (around 15% tree cover). White areas in the study area indicate regions influenced by human activities. **b**, Long-term rainfall variability. The variability is divided into four climatic regions, referred to as very high, high, low and very low rainfall variability, based on the percentiles of the PCA values. The hatched areas illustrate the arc of bistability, that is, regions with precipitation regimes in which both forest and savannah can be sustained (1,300 mm yr^{-1} < MAP < 2,100 mm yr^{-1}).

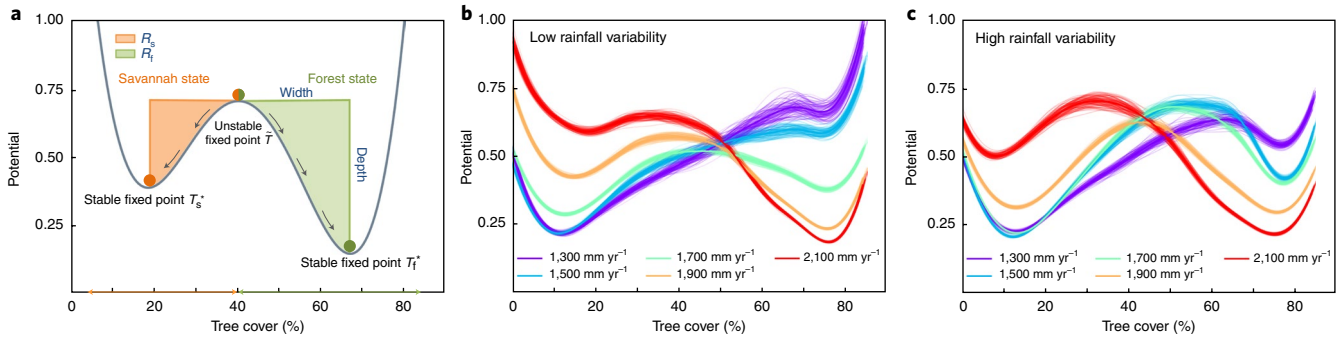

Fig. 2 | Potential of tree cover fractions for different precipitation regimes. a, Conceptual figure that illustrates different stability properties. The grey curve shows the potential wells for the two vegetation states and the unstable state between them. The width and depth of a potential can be used to quantify the stability of the vegetation state. As an overall measure the resilience *R* is introduced here based on the volume of the potential well. **b**,**c**, For the study area, the potentials are derived for different MAP levels for low (**b**) and high (**c**) long-term rainfall variability. Each level shows an ensemble of potentials based on Monte Carlo sampling for each MAP value (Supplementary Methods 2).

substitution approach. We calculated the probability density functions of the tree cover fractions for distinct MAP values (Supplementary Fig. 4). For the different values of MAP, the distributions exhibit either one or two maxima, which correspond to savannah (with a tree cover fraction of 5–20%) and forest (with a tree cover fraction around 70–85%), respectively. This definition of savannah and forest is consistent with that of previous studies[10,15] and other land cover data sets (compare Fig. 1a and Supplementary Figs. 5 and 6).

From each probability density function, we derived the respective potential[21] well (Supplementary Methods 2 and Supplementary Fig. 4). The potential's minima correspond to maxima of the probability distribution and represent stable vegetation states, that is, stable fixed points. Potential wells represent the domain of attraction for a given stable state, that is, they show how much oscillation and perturbation a system can absorb without transitioning to an alternative state[20] (Fig. 2). In our case, collapse may occur if perturbations, such as fires, extreme droughts or deforestation, push forest ecosystems across the unstable fixed point (that is, the potentials maximum between the minima) towards the savannah state. To ensure that the shape of the potentials does not depend on the particular spatial sample region, we estimated an ensemble of potentials from Monte Carlo sampled subsets of grid cells from the study area.

Estimating the resilience of forest and savannah

Various measures have been introduced to estimate the resilience of vegetation[22]. Theoretical work on general dynamical system stability mainly focuses on local measures[23]. Recently, this was complemented by the global concept of basin stability[24], which corresponds to the width of the potential well in question (Methods and Supplementary Figs. 7 and 8). To assess fully the resilience of each vegetation state, we propose the usage of the volume of the potential well as a resilience measure *R*, that is, the combination of both the width and the depth of the well (shaded areas in Fig. 2a (Methods)). Such a measure *R* provides an intuitive interpretation in terms of the time the system will stay in a given vegetation state when exposed to external perturbations[25]. This definition of resilience thus integrates the above, previously introduced measures into a global measure of vegetation resilience that includes the ability to withstand pulse-like disturbances, such as extreme droughts or fires, but also the gradually changing climate conditions.

Generally, we found that the resilience of both forest and savannah is strongly modulated by rainfall variability: in the bistable MAP range, where both savannah and forest can exist, the potential wells are overall wider and deeper in regions where higher rainfall variability occurs (Fig. 2b,c). This indicates the prevalence of a compensation mechanism that increases resilience in places where vegetation is embedded within a more variable rainfall environment.

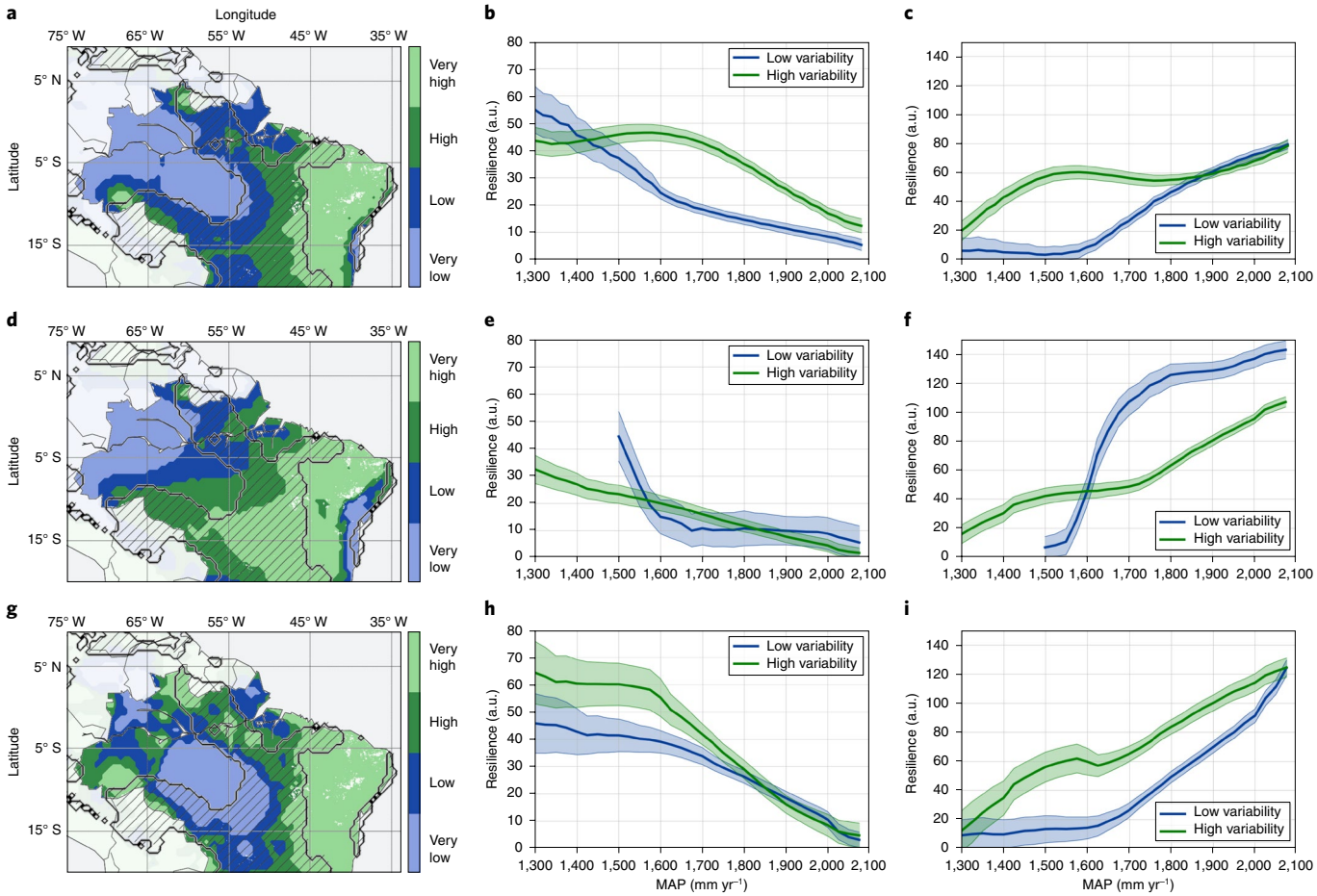

Fig. 3 | Resilience of savannah and rainforest for different precipitation regimes. a,**d**,**g**, The spatial distribution of the variability zones, that is, rainfall variability (**a**), seasonality (**d**) and interannual variability (**g**). **b**–**i**, The resilience of the two intermediate variability regimes for savannah (**b**, **e** and **h**) and forest (**c**, **f** and **i**) as a function of MAP. The two sigma bands (shading) indicate uncertainties derived from Monte Carlo sampling (Supplementary Methods 2). The hatched areas illustrate the bistable MAP regime (1,300 mm yr^{-1} < MAP < 2,100 mm yr^{-1}). Regions that experience stronger rainfall variability (green curves) have generally a higher resilience, except for forest in regions with strong seasonality (the text gives details). a.u., arbitrary units.

Higher rainfall variability may increase tree cover resilience because it potentially drives the selection of vegetation adaptive traits (for example, traits conducive to higher drought resistance or higher diversity of hydraulic traits) to water deficits. In other words, higher rainfall variability might act as a strong environmental filter on vegetation properties and exert a 'training effect' towards higher resilience.

The processes that determine such increments in resilience are so far not fully understood, but are probably linked to functional characteristics of the vegetation. Field measurements at sites in South and Central America, for example, yield a significant positive correlation between vegetation drought sensitivity and total precipitation amounts[25–27]. In addition, more drought-resistant seedlings are dominant in drier regions of the tropics[28]. At the local scale, Amazon forests under more stable hydrological conditions and with more constant access to the water table tend to invest less in hydraulic safety and are more drought sensitive. This suggests that environmental conditions shape the vegetation over the course of centuries[29–31]. This environmental filtering[32] mechanism, which favours more drought-resistant taxa, may explain the overall increase in resilience under higher rainfall variability regimes that we detect for both forest and savannah (Fig. 3b,c). Alternatively, higher rainfall variability regimes might favour the persistence of tree communities with a higher diversity of hydraulic or other functional traits, which might also increase the resilience of the ecosystems[33].

We further separated the impact of the two parameters that form rainfall variability, that is, seasonality and interannual variability (Fig. 3). Seasonality in the study region generally increases along a northwestern–southeastern diagonal, and is low along the coastline (Fig. 3d). However, the spatial distribution of the interannual variability shows lower values in the central Amazon, which increase towards eastern Brazil (Fig. 3g). The effect of a change in seasonality on the resilience of savannah is marginal (Fig. 3e), whereas low seasonality favours a more resilient forest (Fig. 3f). The interannual variability, on the contrary, has an enhancing effect on the resilience of both savannah and forest (Fig. 3h,i). The contrasting effects of seasonality and interannual variability on forest can be explained by the fact that rainforest is mostly favoured in regions without extensive seasonality, and if rainforest is nevertheless found in such regions, it exhibits a lower resilience. However, high interannual variability substantially strengthens the resilience of the rainforest. Comparing these results to the dependency on the overall rainfall variability (Fig. 3b,c), we infer that interannual variability might allow windows of opportunities for the establishment of tree species with contrasting hydraulic traits, which increases the overall hydraulic diversity that leads to a higher vegetation resilience. Beyond a threshold of about 2,100 mm yr^{-1} of MAP,

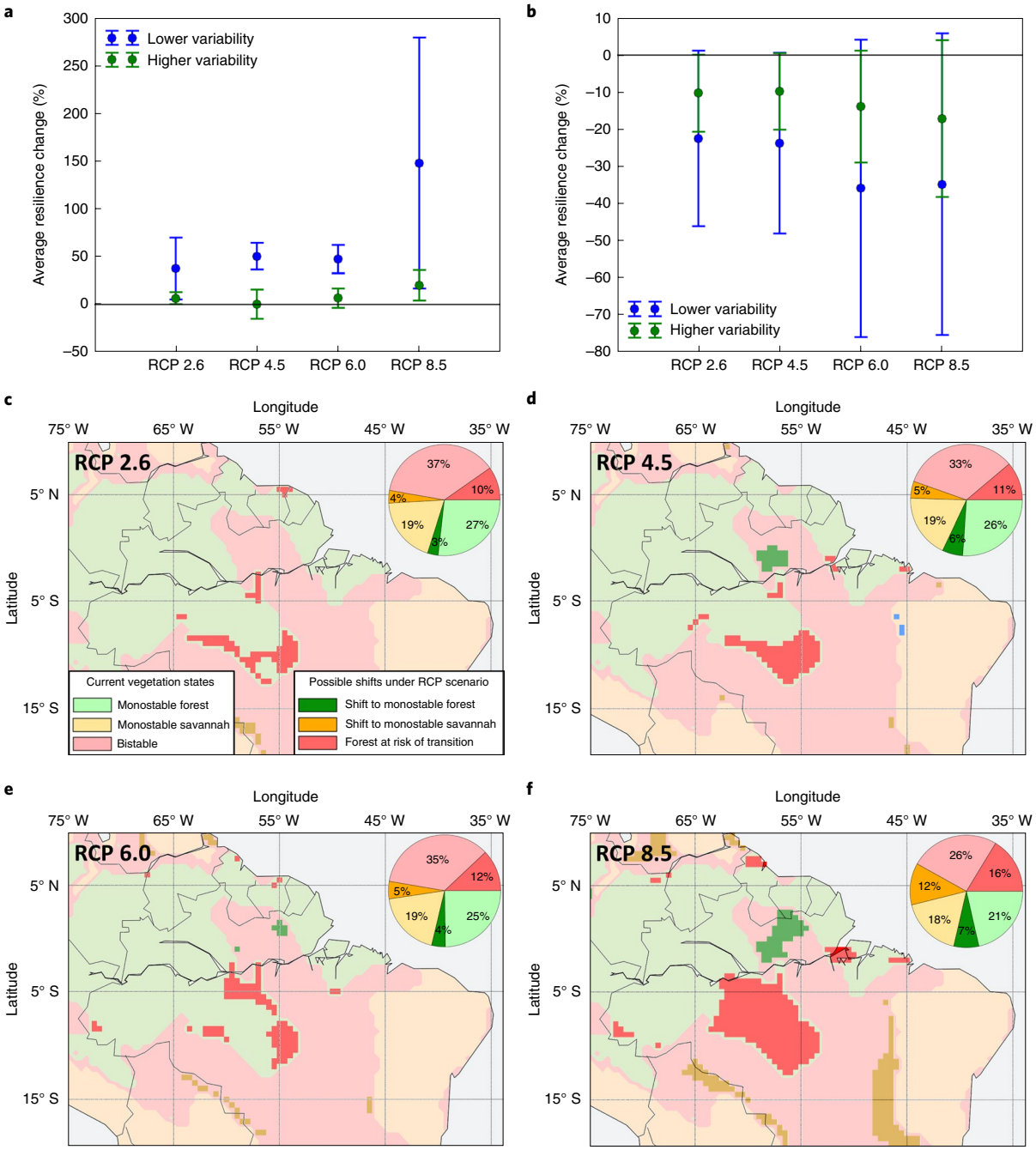

Fig. 4 | Potential shifts of vegetation states under future climate change. a,**b**, For each climate scenario (RCP), the median of the relative change in resilience of savannah (**a**) and rainforest (**b**) imposed by the total MAP change is computed for the time period 2090–2100, compared with 1990–2000. The error bars indicate the variance of resilience change in the models used. **c**–**f**, The maps show the current monostable forest and savannah vegetation regimes as well as the bistable one in the light shading. Additionally, probable transitions between vegetation states emerge due to changes in MAP under the corresponding RCP scenarios, illustrated in dark colours. Each pie chart gives the 2100 distribution in the corresponding scenario (Supplementary Methods 4).

forest is stable irrespective of the rainfall variability. The combination of the amount of annual rainfall and its variability during the long-term past thus strongly influences the resilience of the current vegetation cover.

Future scenarios

With progressing climate change, climate models based on the representative concentration pathway (RCP) emission pathways[34] project a general decrease of MAP in tropical Brazil[17] (Supplementary Fig. 9 and Supplementary Methods 4). At the same time, floods and droughts are likely to become more frequent and more intense. These changes will have a strong influence on the tropical vegetation. In this context, the effect of long-term rainfall variability in modulating the resilience of rainforest and savannah will become even more crucial. We used climate projections from global climate models to explore the impact of changes in MAP on the resilience of Amazon ecosystems. Our results suggest that the projected decline in MAP for higher emission scenarios will lead to a gradual loss of

resilience of the rainforest in the next decades. We found that this effect would more than double in regions that have experienced low rainfall variability in their past (Fig. 4a,b). In addition, the expected precipitation decrease will lead to more favourable conditions for savannah, which would in turn become more stable. However, we emphasize that we here only consider projected changes in MAP to assess the potential loss or gain of resilience under climate change until the year 2100. We do not explicitly consider here the corresponding increase in surface air temperature, which projections show to be homogeneous in tropical South America and thus would not significantly alter our results. Furthermore, we assume that the projected changes in rainfall variability are not going to have a significant environmental filtering effect on vegetation on such short timescales. Based on the projected changes in MAP, we can identify critical regions in which the vegetation is most prone to switching into a different state (Fig. 4c–f). In particular, we emphasize a large coherent region in the southern Amazon that is likely to be under risk of transition from forest to savannah due to the projected reduction of MAP. As this is a lower-variability region, it will be particularly vulnerable to severe droughts.

We uncover that the critical precipitation regimes at which a dieback of the Amazon rainforest might occur depend crucially on the stabilizing effect of long-term rainfall variability. Longer, large-scale observational data and field data are needed to understand further the physiological and ecological processes that underlie the compensation mechanism revealed here and to assess the dynamics of the Amazon rainforest under ongoing global warming. In principle, our approach to estimate vegetation resilience and its preconditioning through rainfall variability can be extended to other tropical regions. However, this requires highly resolved, large-scale data sets that indicate land use areas and vegetation types to avoid biases. Although long-term rainfall variability turns out to be a crucial indicator for the resilience of forest and savannah, other environmental variables, such as temperature distribution[35], different soil types[36] and biodiversity[37] have a strong influence on the vegetation state as well, and need to be closely monitored to assess their impact on resilience. In addition to these climate disturbances, the Amazon rainforest is threatened by large-scale deforestation. Especially in regions within the bistable rainfall regime, large fractions of natural vegetation have already been converted into pasture and agricultural land. Deforestation, even of rather small parts of the rainforest, leads to non-linear feedbacks that reduce the amount of precipitation in South America, and may therefore increase the overall vulnerability of the Amazon rainforest[38–40].

Online content

Any methods, additional references, Nature Research reporting summaries, source data, statements of data availability and associated accession codes are available at https://doi.org/10.1038/s41561-019-0312-z.

Received: 13 November 2017; Accepted: 21 January 2019;
Published online: 25 February 2019

References

1. Malhi, Y. et al. Exploring the likelihood and mechanism of a climate-change-induced dieback of the Amazon rainforest. *Proc. Natl Acad. Sci. USA* **106**, 20610–20615 (2009).
2. Huntingford, C. et al. Simulated resilience of tropical rainforests to CO_2-induced climate change. *Nat. Geosci.* **6**, 268–273 (2013).
3. Rammig, A. et al. Estimating the risk of Amazonian forest dieback. *New Phytol.* **187**, 694–706 (2010).
4. Rowland, L. et al. Death from drought in tropical forests is triggered by hydraulics not carbon starvation. *Nature* **528**, 119–122 (2015).
5. McDowell, N. G. & Allen, C. D. Darcy's law predicts widespread forest mortality under climate warming. *Nat. Clim. Change* **5**, 669–672 (2015).
6. Cox, P. M., Betts, R. A., Jones, C. D., Spall, S. A. & Totterdell, I. J. Acceleration of global warming due to carbon-cycle feedbacks in a coupled climate model. *Nature* **408**, 184–187 (2000).
7. Staal, A., Dekker, S. C., Xu, C. & van Nes, E. H. Bistability, spatial interaction, and the distribution of tropical forests and savannahs. *Ecosystems* **19**, 1080–1091 (2016).
8. Holling, C. S. Resilience and stability of ecological systems. *Annu. Rev. Ecol. Syst.* **4**, 1–23 (1973).
9. Gunderson, L. H. Ecological resilience—in theory and application. *Annu. Rev. Ecol. Syst.* **31**, 425–439 (2000).
10. Hirota, M., Holmgren, M., Van Nes, E. H. & Scheffer, M. Global resilience of tropical forest and savanna to critical transitions. *Science* **334**, 232–235 (2011).
11. Hilker, T. et al. Vegetation dynamics and rainfall sensitivity of the Amazon. *Proc. Natl Acad. Sci. USA* **111**, 041–16,046 (2014).
12. Xu, X. et al. Tree cover shows strong sensitivity to precipitation variability across the global tropics. *Glob. Ecol. Biogeogr.* **27**, 450–460 (2018).
13. Flores, B. M. et al. Floodplains as an Achilles' heel of Amazonian forest resilience. *Proc. Natl Acad. Sci. USA* **114**, 4442–4446 (2017).
14. Anderegg, W. R. et al. Tree mortality predicted from drought-induced vascular damage. *Nat. Geosci.* **8**, 367–371 (2015).
15. Staver, A. C., Archibald, S. & Levin, S. A. The global extent and determinants of savanna and forest as alternative biome states. *Science* **334**, 230–232 (2011).
16. Holmgren, M., Hirota, M., van Nes, E. H. & Scheffer, M. Effects of interannual climate variability on tropical tree cover. *Nat. Clim. Chang* **3**, 755–758 (2013).
17. Magrin, G. O. et al. in *Climate Change 2014: Impacts, Adaptation, and Vulnerability* (eds Field, C. B. et al.) 1499–1566 (IPCC, Cambridge Univ. Press, 2014).
18. Hansen, M. C. et al. Global percent tree cover at a spatial resolution of 500 meters: first results of the MODIS vegetation continuous fields algorithm. *Earth Interact.* **7**, 1–15 (2003).
19. Harris, I., Jones, P. D., Osborn, T. J. & Lister, D. H. Updated high-resolution grids of monthly climatic observations—the CRU TS3.10 dataset. *Int. J. Climatol.* **34**, 623–642 (2014).
20. Scheffer, M. & Carpenter, S. R. Catastrophic regime shifts in ecosystems: linking theory to observation. *Trends Ecol. Evol.* **18**, 648–656 (2003).
21. Livina, V. N., Kwasniok, F. & Lenton, T. M. Potential analysis reveals changing number of climate states during the last 60 kyr. *Clim. Past Discuss.* **6**, 77–82 (2010).
22. Scheffer, M., Carpenter, S. R., Dakos, V. & van Nes, E. H. Generic indicators of ecological resilience: inferring the chance of a critical transition. *Annu. Rev. Ecol. Evol. Syst.* **46**, 145–167 (2015).
23. Walker, B., Holling, C. S., Carpenter, S. R. & Kinzig, A. Resilience, adaptability and transformability in social–ecological systems. *Ecol. Soc.* **9**, 5 (2004).
24. Menck, P. J., Heitzig, J., Marwan, N. & Kurths, J. How basin stability complements the linear-stability paradigm. *Nat. Phys.* **9**, 89–92 (2013).
25. Engelbrecht, B. M. J. et al. Drought sensitivity shapes species distribution patterns in tropical forests. *Nature* **447**, 80–82 (2007).
26. Esquivel-Muelbert, A. et al. Seasonal drought limits tree species across the neotropics. *Ecography* **40**, 618–629 (2017).
27. Esquivel-Muelbert, A. et al. Biogeographic distributions of neotropical trees reflect their directly measured drought tolerances. *Sci. Rep.* **7**, 1–11 (2017).
28. Poorter, L. & Markesteijn, L. Seedling traits determine drought tolerance of tropical tree species. *Biotropica* **40**, 321–331 (2007).
29. Cosme, L. H. M., Schietti, J., Costa, F. R. C. & Oliveira, R. S. The importance of hydraulic architecture to the distribution patterns of trees in a central Amazonian forest. *New Phytol.* **215**, 113–125 (2017).
30. Rogers, B. M., Soja, A. J., Goulden, M. L. & Randerson, J. T. Influence of tree species on continental differences in boreal fires and climate feedbacks. *Nat. Geosci.* **8**, 228–234 (2015).
31. Oliveira, R. S. et al. Embolism resistance drives the distribution of Amazonian rainforest tree species along hydro-topographic gradients. *New Phytol.* **221**, 1457–1465 (2019).
32. Walker, B. & Salt, D. *Resilience Thinking: Sustaining Ecosystems and People in a Changing World* (Island Press, Washington DC, 2012).
33. Anderegg, W. R. L. et al. Hydraulic diversity of forests regulates ecosystem resilience during drought. *Nature* **561**, 538 (2018).
34. van Vuuren, D. P. et al. The representative concentration pathways: an overview. *Climatic Change* **109**, 5–31 (2011).
35. Anderegg, W. R. L. et al. The roles of hydraulic and carbon stress in a widespread climate-induced forest die-off. *Proc. Natl Acad. Sci. USA* **109**, 233–237 (2012).
36. Guidão, P., Ruggiero, C., Batalha, M. A. & Pivello, V. R. Soil–vegetation relationships in cerrado (Brazilian savanna) and semideciduous forest, Southeastern Brazil. *Plant Ecol.* **60**, 1–16 (2002).
37. Sakschewski, B. et al. Resilience of Amazon forests emerges from plant trait diversity. *Nat. Clim. Change* **6**, 1032–1036 (2016).

38. Boers, N., Marwan, N., Barbosa, H. M. J. & Kurths, J. A deforestation-induced tipping point for the South American monsoon system. *Sci. Rep.* **7**, 1–9 (2017).
39. Lawrence, D. & Vandecar, K. Effects of tropical deforestation on climate and agriculture. *Nat. Clim. Change* **5**, 27–36 (2015).
40. Zemp, D. C. et al. Self-amplified Amazon forest loss due to vegetation–atmosphere feedbacks. *Nat. Commun.* **8**, 1–10 (2017).

Acknowledgements

We thank S. Lange for providing the global climate model data. We thank E. H. van Nes for the helpful introduction in computing potential landscapes. This paper was developed within the scope of the IRTG 1740/TRP 2015/50122-0, funded by the DFG/FAPESP. C.C. acknowledges the project grant BMBF 01LN1306A. M.H. and R.S.O. acknowledge the project grants Microsoft/FAPESP 2013/50169–1 and 2011/52072-0, as well as Instituto Serrapilheira/Serra-1709–18983. N.B. acknowledges funding by the German Science Foundation (DFG, Reference BO 4455/1–1). R.W. is thankful for support by the Leibniz Association (project DominoES).

Author contributions

C.C., N.B., M.H. and R.W. conceived the study and prepared the manuscript with contributions from R.S.O. C.C. performed the analyses. All the authors discussed the results and contributed to editing the manuscript.

Competing interests

The authors declare no competing interests.

Additional information

Supplementary information is available for this paper at https://doi.org/10.1038/s41561-019-0312-z.

Reprints and permissions information is available at www.nature.com/reprints.

Correspondence and requests for materials should be addressed to C.C. or R.W.

Publisher's note: Springer Nature remains neutral with regard to jurisdictional claims in published maps and institutional affiliations.

Methods

Data. For our analysis, tree cover (T) data were retrieved from the continuous tree cover distribution MOD44B at 250 m resolution for the year 2012 from the MODIS Terra vegetation continuous fields data set[18]. As pointed out in previous studies[41–44], the tree cover data set is not useful for very low amounts of tree cover ($T < 10\%$). Therefore, this study excludes desert-like climatic areas (defined as MAP < 300 mm yr^{-1}) from the analyses. The data set exhibits tree cover percentages between 70 and 85% in areas classified as forest and between 5 and 15% in areas classified as natural pasture and shrubland (savannah) according to the Brazilian Institute of Geography and Statistics (IBGE) (Supplementary Figs. 5 and 6). To guarantee an unbiased analysis, all the regions that are significantly affected by human land use, as derived from the IBGE data set[45], are excluded from the analysis. Such accurate and spatially extensive data on human land use in tropical regions is, to our knowledge, only available for the Brazilian Amazon.

MAP values and long-term rainfall variability are derived from the CRU's high-resolution monthly data CRU TS3.24[19] for the years 1961–2012. It is a state-of-the-art rain gauge product from meteorological stations, interpolated to a regular grid of 0.5° resolution.

Variability analysis. We computed the long-term interannual variability from the CRU precipitation data set as the standard deviation of MAP values divided by their long-term mean, and quantified the seasonality by the Markham seasonality index[46] for each grid cell (Supplementary Methods 1). The seasonality and interannual variability are combined into one measure of overall long-term rainfall variability on the basis of a principal component analysis (PCA) (Supplementary Methods 3). The study area was then categorized into four variability classes. First, negative values of the PCA-derived variability were assigned to a lower variability and positive values to a higher variability. These two classes were further subdivided at their respective medians to obtain four variability classes that ranged from a very high (50th to 100th percentiles) to a high (0th to 50th percentiles) variability for positive PCA values, and from low (0th to 50th percentiles) to very low (50th to 100th percentiles) variability for negative PCA values. This classification was used to determine the long-term rainfall variability zones used in this study. For the classification of the variability zones of seasonality and interannual variability, we divided the data into four equally sized partitions by computing the 25th, 50th and 75th percentiles. Values below the 25th percentile were considered as very low variability, those between the 25th and 50th percentiles as low variability, those between the 50th and 75th percentiles as high variability and those above the 75th percentile as very high variability.

Stability measures. To quantify different aspects of the stability of a vegetation state, various measures were introduced, mainly based on the width w and depth d of the potential well that corresponds to the vegetation state (Fig. 2a). Here the width is defined as the horizontal distance between the stable fixed point of the state in question and the unstable fixed point that marks the boundary to the alternative state. Analogously, the depth is determined as the vertical distance between these two points. In this study, we compared the following measures:

- The width w of the potential well, also referred to as the latitude[23]. This quantifies the maximum size of a single perturbation in tree cover, such that the system is still able to recover to its original stable state. This is similar to the recently introduced concept of basin stability[24].
- The depth d, also referred to as the resistance. It has been argued that this quantifies the difficulty of moving the system away from its current stable state[23,47].
- The local Lyapunov stability[48], defined here as the local Lyapunov exponent at the fixed point in question, that is, the minimum of the potential well: This is a standard local stability measure in dynamical systems theory that quantifies the effort needed to bring the system out of equilibrium.

All of these measures are limited to different, specific aspects that characterize the stability of the system state. By considering the two-dimensional volume of the potential well, we combines these different aspects into one global measure of vegetation stability, which we call resilience (R):

- For both the savannah (s) and forest (f) states, we defined their resilience $R_{s/f}$ as the volume of that part of the corresponding potential well that lies between the respective stable fixed point (T_s^* and T_f^*, respectively) and the unstable fixed point ($\widetilde{T}$) that separates the two wells (shaded areas in Fig. 2a). Formally, for tree cover denoted by T and potential U_p, we defined $R_{s/f}$ as:

$$R_s = \int_{T_s^*}^{\widetilde{T}} \mathrm{d}T[U_p(\widetilde{T}) - U_p(T)]$$

and

$$R_f = \int_{\widetilde{T}}^{T_f^*} \mathrm{d}T[U_p(\widetilde{T}) - U_p(T)]$$

So, $R_{s/f}$ is directly related to the so-called mean first passage time of the associated Fokker–Planck equation[49]. It thus provides a general and intuitive measure of vegetation stability in terms of the time the system will stay within the respective potential well when exposed to external, noisy perturbations.

Therefore, $R_{s/f}$ suits as an approximation for the stability of the system's state, in particular against abrupt disturbances such as droughts or fires, but also against continuously changing external conditions, such as global warming and the associated changes, for example, in rainfall and drought frequency.

Climate scenarios. We considered MAP changes under the RCP[34] future emission scenarios, as projected by the global climate models GFDL-ESM2M, HadGEM2-ES, MIROC-ESM-CHEM, IPSL-CM5A-LR and NorESM1-M. We took the gridded climate data from the ISIMIP Fast Track input-data catalogue[50,51]. The original data were retrieved from the CMIP5 archive and bias corrected[50] for the CRU precipitation data set. We used the median of the five models for all the analyses.

Code availability

The computer code used for this study is available on request.

Data availability

The data reported in this paper are extracted from the publicly available sites of MODIS (https://lpdaac.usgs.gov/)[52], IBGE (https://www.ibge.gov.br/)[45] and CRU (https://crudata.uea.ac.uk/)[19].

References

41. Staver, A. C. & Hansen, M. C. Analysis of stable states in global savannas: is the CART pulling the horse? A comment. *Glob. Ecol. Biogeogr.* **24**, 985–987 (2015).
42. Hanan, N. P., Tredennick, A. T., Prihodko, L., Bucini, G. & Dohn, J. Analysis of stable states in global savannas: is the CART pulling the horse? *Glob. Ecol. Biogeogr.* **23**, 259–263 (2014).
43. Hanan, N. P., Tredennick, A. T., Prihodko, L., Bucini, G. & Dohn, J. Analysis of stable states in global savannas—a response to Saver and Hansen. *Glob. Ecol. Biogeogr.* **24**, 988–989 (2015).
44. Gerard, F. et al. MODIS VCF should not be used to detect discontinuities in tree cover due to binning bias. A comment on Hanan et al. (2014) and Staver and Hansen (2015). *Glob. Ecol. Biogeogr.* **26**, 854–859 (2017).
45. *Cobertura e uso da terra 2012* (IBGE, accessed 3 February 2019); ftp://geoftp.ibge.gov.br/informacoes_ambientais/cobertura_e_uso_da_terra/mudancas/vetores/
46. Markham, C. G. Seasonality of precipitation in the United States. *Ann. Assoc. Am. Geogr.* **60**, 593–597 (1970).
47. Pimm, S. L. The complexity and stability of ecosystems. *Nature* **307**, 321–326 (1984).
48. Mitra, C., Kurths, J. & Donner, R. V. An integrative quantifier of multistability in complex systems based on ecological resilience. *Sci. Rep.* **5**, 16196 (2015).
49. Gardiner, C. *Handbook of Stochastic Methods for Physics, Chemistry and the Natural Sciences* (Springer, Berlin, 2004).
50. Hempel, S., Frieler, K., Warszawski, L., Schewe, J. & Piontek, F. A trend-preserving bias correction—The ISI-MIP approach. *Earth Syst. Dyn.* **4**, 219–236 (2013).
51. Warszawski, L. et al. The Inter-Sectoral Impact Model Intercomparison Project (ISI–MIP): project framework. *Proc. Natl Acad. Sci. USA* **111**, 3228–3232 (2014).
52. Dimiceli, C. et al. *MOD44B MODIS/Terra Vegetation Continuous Fields Yearly L3 Global 250 m SIN Grid V006* (NASA EOSDIS Land Processes DAAC, 2015); https://doi.org/10.5067/MODIS/MOD44B.006